Finja Borowski\*, Stefan Siewert, Klaus-Peter Schmitz, Michael Stiehm, and Daniela Koper

# Lumen reconstruction of covered stents for numerical simulation of thrombosis risk

https://doi.org/10.1515/cdbme-2025-0205

**Abstract:** Covered stents are increasingly used in the treatment of aortoiliac occlusions and aneurysms. However, the presence of a polymeric cover may inhibit endothelialization and alter blood flow, potentially increasing the risk of thrombosis. Accurate geometric models of the stent lumen are crucial for computational fluid dynamics (CFD) simulations for thrombosis risk assessment. This study presents a workflow combining silicone casting,  $\mu$ CT imaging, and CFD for thrombosis risk assessment. Applied to a Gore Viabahn VBX stent, the workflow achieved high accuracy with deviations below 0.1 mm. CFD simulations identified low wall shear stress regions downstream of cover-induced constrictions, critical for thrombus formation. This approach offers valuable insights for stent design optimization.

**Keywords:** Covered stent lumen reconstruction, CFD, thrombosis risk

### 1 Introduction

Covered stents are essential for treating aortoiliac occlusions, stenosis, and aneurysms [1]. They consist of a metallic scaffold with a polymeric cover providing an impermeable barrier against blood leakage. Their minimally invasive deployment has led to widespread adoption, with recommendations as a first-line treatment for aortoiliac occlusive disease [2]. Despite their success, polymeric covers can hinder endothelialization, increasing thrombosis risk [3]. Furthermore, it is known from the coronary artery domain that the blood flow inside a covered stent can be significantly altered due to the presence of the cover and the struts of the stent. These alterations can lead to changes in flow patterns and even turbulence, which in turn may influence thrombus formation and restenosis [4]. Thus, understanding and optimizing the hemodynamic environment within covered stents is critical for improving their design and long-term patency.

Computational fluid dynamics (CFD) simulations have become a powerful tool in the evaluation and optimization of

\*Corresponding author: Finja Borowski, Institute for ImplantTechnology and Biomaterials, Friedrich-Barnewitz-Straße 4, Rostock, Germany, e-mail: finja.borowski@iib-ev.de Stefan Siewert, Klaus-Peter Schmitz, Michael Stiehm, Daniela Koper, Institute for ImplantTechnology and Biomaterials, Rostock, Germany

stents, as they allow for the detailed assessment of hemodynamic parameters, such as wall shear stress (WSS), which is a key indicator for thrombotic risk. Stagnation zones characterized by low WSS can promote platelet aggregation and fibrin deposition, increasing the likelihood for thrombus formation [5]. To accurately perform such simulations, a precise geometric model of the post-implantation lumen is necessary.

Imaging techniques, such as contrast-enhanced computed tomography (CT), have been employed to reconstruct the lumen of covered stents for *in vitro* and *in silico* analyses. However, due to the high radiopacity of the metallic stent frame, imaging artifacts often hinder accurate lumen segmentation [6], as examplarly shown in Fig. 1 for a covered stent.

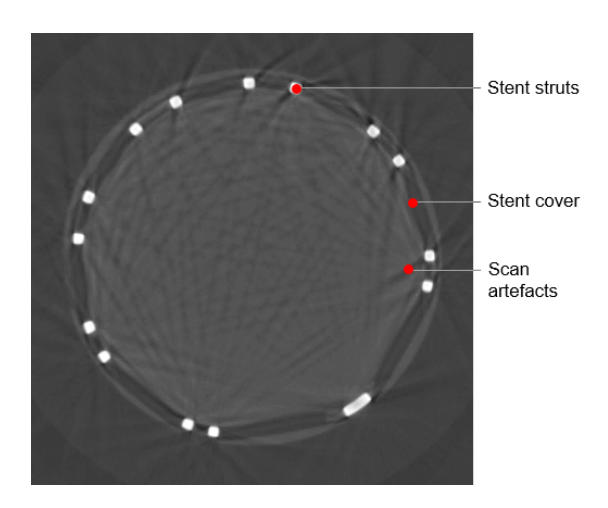


Fig. 1: Cross-section image reconstructed from  $\mu$ CT-scan of the covered stent and iodium solution with artefacts.

To overcome this limitation, this study presents a novel methodology for lumen reconstruction using silicone casting,  $\mu$ CT imaging, and numerical flow simulations. The proposed workflow enables the generation of detailed lumen geometries, which can subsequently be utilized for CFD-based thrombosis risk assessment. By integrating experimental and numerical approaches, this study aims to enhance the understanding of flow dynamics in covered stents and contribute to the development of next-generation endovascular devices.

### 2 Material und Method

The workflow for reconstruction of the vessel lumen and simulation of the flow through a covered stent is demonstrated in this study using a commercially available stent. The Gore Viabahn VBX stent (W. L. Gore & Associated Inc., USA) with a nominal diameter of 10 mm and a length of 59 mm was used.

Several steps were performed to reconstruct the stent lumen: Step 1: Implantation of the covered stent into a vessel model. Step 2: Pouring the stent in the vessel model with silicone. Step 3:  $\mu$ CT scan of the silicone imprint of the lumen. Step 4: Reconstruction of a 3D lumen model.

A silicone tube with a diameter of 10 mm and a wall thickness of 1 mm was used as vessel model. Before the stent implantation was performed, the silicone tube was sprayed with a release coating (Achem SG-10008S, Angewandte Chemie GmbH, GER). The stent was expanded to nominal diameter at nominal pressure (11 atm) in the vessel model using a ballon catheter in accordance to the instruction for use.

A two-component silicone elastomer (Sylgard 184 Silicone Elastomer, Dow Chemical Company, USA) was used to mold the lumen geometry. The silicone was cured at 80 °C for 24 hours. The silicone cast was then detached from the vessel model and the covered stent, see Fig. 2.

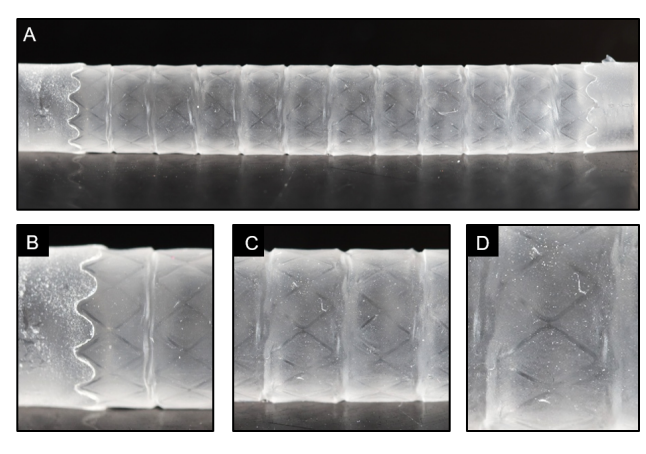


**Fig. 2:** Silicone cast of the Viabahn VBX stent (A) in its entire length, (B) detailed view of the beginning of the stent, (C) detailed view of the individual stent segments and the constrictions between them and (D) the surface of the silicone in which the struts are imprinted.

The silicone model of the lumen was next analyzed using  $\mu$ CT scan (SkyScan1273, Bruker Corp., USA). The scan was conducted using a resolution of  $7 \mu m$  per voxel. The recordings were reconstructed in cross-section slices using NRecon. The cross-section slices were also binarized and smaller area were eliminated using the despeckle filter in post-processing.

Finally, a 3D geometric model of the lumen was created from the processed images and is shown in Fig. 3.

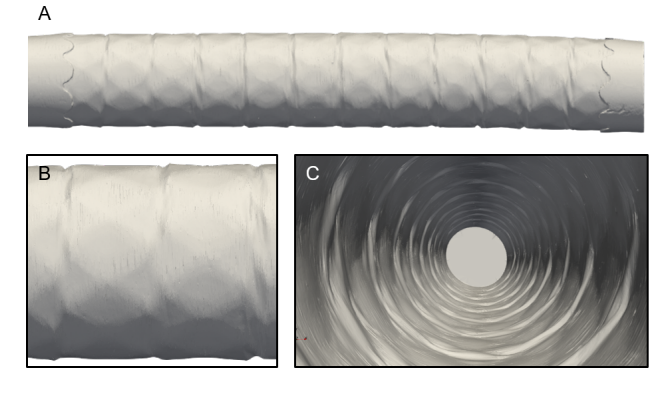


Fig. 3: Reconstructed lumen model of the Viabahn VBX in (A) general view, (B) detailed view of two stent segments and the constriction of the cover between them and (C) internal view of the model, in which the constriction of the cover between the stent segments can be seen.

The geometry model was then used for numerical flow simulations. In order to ensure the best possible mesh quality, the geometry model of the lumen was smoothed using a smoothing and shrinkwrap algorithm with the SpaceClaim (Ansys Inc., USA) and then remeshed in Fusion 360 (Autodesk Inc., USA). A circular inlet and outlet section were also added to the geometry model, each corresponding to the stent length. The fluid domain was mainly meshed with hexaeder elements, resulting in a mesh with 11.4 million elements. The flow simulations were performed with openFOAM v2406 software package (OpenCFD Ltd., UK). The Carreau-Yasuda viscosity model was used to obtain the non-Newtonian properties of blood. The parameters for the model were determined according to Cho and Kensey [7]. The density of the fluid was  $1060 \,\mathrm{kg} \,\mathrm{m}^{-3}$ . A parabolic velocity profile with an average flow velocity of  $0.5 \,\mathrm{m\,s^{-1}}$  was specified as inlet boundary condition. A no slip boundary condition was defined at the lumen walls and a reference pressure of 0 Pa was defined at the outlet. The simpleFoam solver was used for the numerical cal-

For the assessment of the risk of thrombosis or restenosis, the WSS as well as the residence time (RT) and shear rate (SR) were used. Both the WSS and the SR were derived directly from the calculated velocity field. The RT was implemented into the solver, as already shown in Stiehm et al. [8] and initially proposed by Ghirelli and Leckner [9], with the following scalar transport equation:

$$\frac{\partial RT}{\partial t} + \vec{u} \cdot \nabla RT = 1 \tag{1}$$

### 3 Results and Discussion

The results of the workflow shown in this study are divided into two categories. One is the reconstruction of the lumen geometry of covered stents and the other is the flow simulation and the metrics derived from it to assess the risk of thrombosis or restenosis.

As already shown in Fig. 2, it is possible to create a detailed mold of the lumen geometry using the silicone casting technique. The detailed view in Fig. 2 B shows one end of the stent, in which the covered meander structures of the stent and the reduction in cross-section due to the stent are clearly visible. In the detailed view of Fig. 2 C it can also be seen how the cover between the stent segments constricts and thus reduces the lumen in this area. Finally, even the individual stent struts can be identified in the silicon mold, see detailed view Fig. 2 D.

The resulting virtual model of the lumen geometry has also already been shown in Fig. 3. A comparison between the virtual model and the silicone casting model shows that the geometry can be accurately reproduced with the  $\mu$ CT scan and the subsequent reconstruction. For comparison, the mean diameter of the model was identified for the silicone model using automated laser scanning determination (ALSD) and for the virtual model at three different cross-sections, see Tab. 1 and 4 (A: at the beginning of the stent; B: lumen in the stent segment region; C: lumen between two stent segments). The ALSD was performed using a 2-axis laser scanner (ODAX 64XY, Zumbach Elektronik AG, Switzerland, measurement accuracy  $\pm$  0.14 % of the measured value).

**Tab. 1:** Average diameter of the cross-section A-C for the real lumen geometry and the reconstructed lumen geometry model.

Cross-section	ALSD diameter	reconstruction diameter
A	$9.48\mathrm{mm}$	$9.47\mathrm{mm}$
В	$9.39\mathrm{mm}$	$9.37\mathrm{mm}$
C	$9.15\mathrm{mm}$	$9.09\mathrm{mm}$

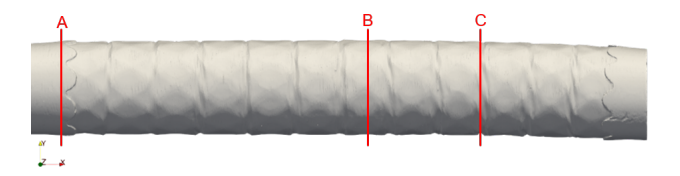


**Fig. 4:** Cross-sections of the stent lumen geometry for (A) lumen at the beginning of the stent; (B) lumen in the stent segment region and (C) lumen between two stent segments.

The second part of the results in this sutdy is the calculated velocity field of the geometry, shown in Fig. 5. As can be seen, the vessel flow is only minimally disturbed by the covered stent. The highest velocities occur in the center of the vessel and are approximately twice the specified mean flow velocity ( $u_{mean} = 0.5 \text{ m s}^{-1}$ ;  $u_{max} = 0.1 \text{ m s}^{-1}$ ).

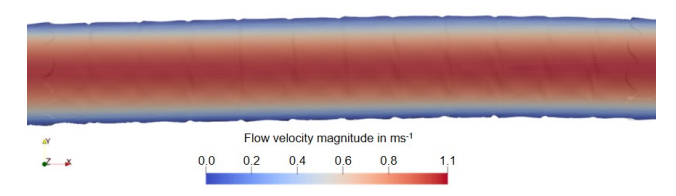


Fig. 5: Flow velocity magnitude inside the covered stent lumen in the longitudinal mid-section.

The WSS is calculated from the flow field and is shown in Fig. 6. According to Malek et al., areas in which the WSS is <0.4 Pa are particularly susceptible to the deposition of blood components [5]. The areas with low WSS occur immediately downstream of the constrictions of the cover, as well as at the end of the stent, where the cross-section of the lumens widens again. The ratio of the area with low WSS to the total area of the covered stent is 0.92 %.



Fig. 6: Wall shear stress magnitude in the region of the covered stent.

RT was used as a further predictor for thrombosis risk. Since the steady state simulations in openFoam are calculated pseudo-transiently, the absolute RT was normalized to the simulated time to use a relative RT as a comparable thrombosis risk metric. The distribution of RT in a longitudinal section of the fluid domain is shown in Fig. 7.

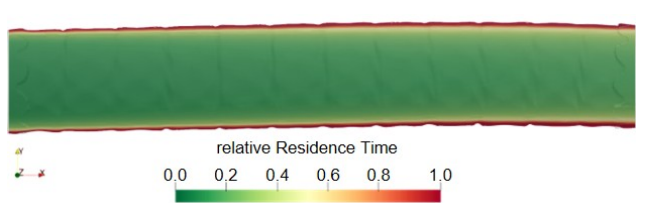


**Fig. 7:** Relative residence time (RT) of the fluid in the region of the covered stent in a longitudinal section.

It can be seen that RT is almost one in the region close to the wall, resulting in a minor fluid exchange in this area. However, if the region with a relative RT of > 0.99 is normalized to the total region of the lumen domain inside the covered stent, the volume of increased RT is only 0.42 % of the total volume.

SR was used as the third predictor for thrombosis risk. The distribution of the SR in a longitudinal section of the fluid domain is shown in Fig. 8. Also shown is a detail view of the SR at the constrictions of the cover in Fig. 8, detail A, where the highest SR also occur. The shear flow affects platelet behavior and thus thrombus formation. It was found that an increased SR ( $> 2200\,\mathrm{s}^{-1}$ ) stimulates the platelets activation [10]. For this reason, this threshold was used to quantify the region with increased SR. However, the fluid volume with increased SR was less than 0.1 % (normalized to the fluid domain within the stent). If the individual metrics are considered in com-

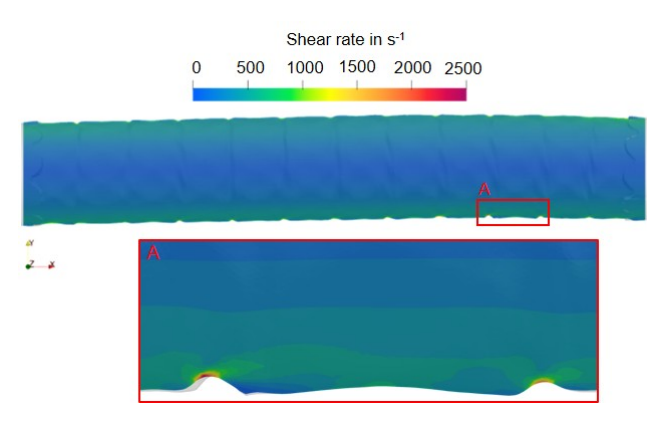


Fig. 8: Distribution of the shear rate (SR) in the longitudinal section of the fluid domain in the stent region.

bination, it is noticable that the increased SR occurs at the cover constrictions between the stent segments. Immediately downstream, there are regions with increased relative RT or areas with low WSS at the lumen wall. This indicates that the constrictions of the cover have a decisive impact on the thrombosis risk of covered stents. While the strut dimensions were the decisive lumen reduction in the field of bare metal or drug eluting stents [11], the cover constrictions could contribute to a significant increase in the risk of thrombosis for covered stents. If the constrictions between stent segments are larger than in case of the Viabahn VBX, the risk of thrombosis could increase significantly. However, this requires further simulations of other products and expansion diameter. Whith this framework, it will be also possible in further investigations to compare covered stent prototypes with commercially available devices in terms of their thrombosis risk.

### 4 Conclusion

The presented approach demonstrates a robust method for reconstructing lumen from covered stents in a vessel model, allowing the generation of high-quality geometry models, which is essential for accurate numerical flow simulations. It was shown that the reconstructed geometry can be used to perform numerical flow simulations to assess the thrombosis risk of covered stents by using wall shear stress, residence time and shear rate.

#### **Author Statement**

Research funding: Financial support by the European Regional Development Fund (ERDF) and the European Social Fund (ESF) within the collaborative research between economy and science of the state Mecklenburg-Vorpommernis is gratefully acknowledged. Conflict of interest: Authors state no conflict of interest.

## References

- [1] A Mallory, S Giannopoulos, and P Lee et al. Covered stents for endovascular treatment of aortoiliac occlusive disease: A systematic review and meta-analysis. *Vasc. Endovasc. Surg.*, 55(6):560–570, 2021.
- [2] V Aboyans, M Björck, and M Brodmann et al. Questions and answers on diagnosis and management of patients with peripheral arterial diseases. *Eur. Heart J.*, 39(9):e35–e41, 2018.
- [3] L Yang, X Hao, and B Gao et al. Endothelialization of ptfecovered stents for aneurysms and arteriovenous fistulas created in canine carotid arteries. *Sci. Rep.*, 14(1):4803, 2024
- [4] N Foin, RD Lee, and R Torii et al. Impact of stent strut design in metallic stents and biodegradable scaffolds. *Int. J. Cardiol.*, 177(3):800–808, 2014.
- [5] AM Malek, SL Alper, and S Izumo. Hemodynamic shear stress and its role in atherosclerosis. *JAMA*, (282(21)):2035– 2042, 1999.
- [6] D Maintz, R Fischbach, and K-U Juergens et al. Multislice ct angiography of the iliac arteries in the presence of various stents: in vitro evaluation of artifacts and lumen visibility. *Invest. Radiol.*, (36(12)):699–704, 2001.
- [7] YI Cho and KR Kensey. Effects of the non-newtonian viscosity of blood on flows in a diseased arterial vessel. part 1: Steady flows. *Biorheology*, (28):241–262, 1991.
- [8] M Stiehm, F Borowski, and S Kaule et al. Computational flow analysis of the washout of an aortic valve by means of eulerian transport equation. *Curr. Dir. Biomed. Eng.*, 5(1):123– 126, 2019.
- [9] F Ghirelli and B Leckner. Transport equation for the local residence time of a fluid. *Chem. Eng. Sci.*, 59(3):513–523, 2004
- [10] H Shankaran, P Alexandridis, and S Neelamegham. Aspects of hydrodynamic shear regulating shear-induced platelet activation and self-association of von willebrand factor in suspension. *Blood*, 101(7):2637–2645, 2003.
- [11] JM Jiménez and PF Davies. Hemodynamically driven stent strut design. *Ann. Biom. Eng.*, 37(8):1483–1494, 2009.